

FILTERING LIDAR POINTS BY FUSION OF INTENSITY MEASURES AND AERIAL IMAGES

J. H. Mao^{a,*}, Q. H. Zeng^a, X. F. Liu^a, J. Z. Lai^b

^aResearch Centre of Remote Sensing and Spatial Information Science, School of Communication and Information Engineering, Shanghai University, 149 Yan Chang Road, Shanghai 200072, China-(mjh,zengqihong,liuxuefeng)@shu.edu.cn

^bThe High School Attached to Jiangxi Normal University, 194 West Beijing Road, Nanchang, Jiangxi China- lili@163.com

Commission III WG III/1

Keywords: LIDAR point data; laser returns intensity; aerial images; returns filtering

Abstract:

Laser return intensity, delivering the surface reflectivity information in the laser wavelength, is function of many variables and ignored in most application projects. However, by a process of SILC (Spectral Imagery LIDAR Composite), laser return points can be fused with accurate spectral attributes from the high quality images provided by aerial cameras on the same board, through which the laser return points have both high quality of reflection properties and geometric information and can be filtered by integrating the reflectivity and intensity method. In this paper, the differences and measurement advantages of reflectivity of laser scanning and aerial images are analyzed, and the similarity of spatial distribution between the laser return intensities and digital numbers of aerial images is obtained by overlapping their images on the DSM of raw LIDAR points. And according to the equivalent reflectivity in the spectral range of red, green and blue of typical land-coverage, laser return points are filtered from the SILC data by the aerial images digital number (DN) parameters. And on the statistic of the filtered return points' intensity, ranges of return intensity for every type of features are obtained, and by which return points are filtered, which is followed by a results discussion.

1. INTRODUCTION

The LIDAR system is an active remote sensing system that utilizes pulsed, single wavelength laser light to measure the distances from the aircraft carrying the LIDAR equipment to points on the terrain from which the laser is reflected. A common LIDAR system is comprised mainly of a laser scanner, a GPS receiver, an inertial navigation system (INS), a group of digital cameras and a cooling system. It transmits very short pulses in the visible or near infrared part of the electromagnetic spectrum by the laser scanner, and record the position and orientation of the aircraft at each transmission of pulse through the GPS and INS. Through the time difference between the transmitted and received pulse, distance to the target can be measured. And by the on-board digital cameras, high resolution aerial images can be obtained simultaneously. Most of the commercial systems allow the recording of multiple echoes from one laser pulse, and some of them deliver not just range but also intensity information, which has been used very little up to now.

Return records from a commercial modern LIDAR system, e.g. the LiteMapper-5600 system, include mainly the return point position (x,y,z coordinates), return number and its times, return intensity, return direction and ranges digital number(DN) of aerial images, etc.. The return intensity delivers the detailed information about the reflectance characteristics of the surface in the laser wavelength, which is typically in the near infrared spectra. Most LIDAR systems recording the intensity are small footprint scanners, which operate with a beam divergence in the range of 0.3 to 0.8 mrad. And the illuminated area covered by the footprint, an approximately circular, is vary strongly with different ranges and scan angles of the laser beam caused by

changes in the flying altitude and the topography of the scanned surface within one flight mission and the emitted laser shot interacts with the objects and generates the backscatter, the intensity of which is function of many variables as the laser power, the double distance source-target, the incidence angle, the reflectivity of the target and the media absorption. Laser power may be vary between different systems, and for its limited lifetime, laser power exhibit a rapid deterioration after long use (Emmanuel,1999). For the scattering and absorption of the laser photons in the atmosphere, the return energy also corresponds to the system-independent atmospheric conditions at the time of flight. For a wavelength of 1060 nm the effect of scattering considerably exceeds the contribution of absorption (Kim et al., 2001). And the noise in the intensity measurement can be around 10%, for the influence of the distribution of intensities in homogeneous regions (Ahokas et al., 2006). And since the distribution of laser energy over the laser footprint is not uniform but Gaussian, the measured backscattered intensity of a target depends also on the position of the target within the laser footprint. And for the uncertainty to it, the return intensity has more or less been an unused byproduct of data collection in most application projects (Jonas, 2002). It is well know that conventional surface classification filters can only go so far when removing above-ground phenomena for it's difficult to determine whether a laser point has hit a special object when only spatial analysis is included. Researchers, however, have shown interest in utilizing the return intensities to deliver more information about the reflecting surfaces than can be derived solely from using LIDAR as a ranging tool (Lim et al., 2003). Schreier et al. (1985) uses intensity measurements, combined with height, for classification of vegetation types, and found that pure broadleaf forests showed reflectance values that are significantly higher than that for pure conifer forests. Jonas

(2002) claims that intensity values may be able to assist in species identification but the correlation between species and laser intensity return pattern is still failed to find. Holmgren and Persson (2004) demonstrated the ability to discriminate between coniferous species, Norway spruce and Scots pine, using six variables including the standard deviation of intensity of all returns. And Jeong-Heon Song et al. (2005) converted LIDAR point data to a grid and assessed the separability of intensity data on some classes, and concluded that LIDAR intensity data could be used for land-cover classification. T. Moffiet et al. (2005) assesses the potential of laser return type and return intensity as variables for classification of individual trees or forest stands according to species by the exploratory data analysis. And with the integration of LIDAR and hyperspectral data, Franco Coren et al. (2005) evaluate irregular behavior of some major ground indexes and improve the method to discovery of new archeological sites. Compared to the returns pulse intensity data, the high quality, large-coverage images provided by aerial cameras is a very important advantage of photogrammetry, which can be a very important complement data source to the LIDAR points cloud. By a process of SILC (Spectral Imagery LIDAR Composite), each surface LIDAR point possesses an accurate spectral signature assigned to its location, allowing accurate classification of features using conventional remote sensing techniques. Through the element of color, SILC data allows features to be subjectively masked and classified, providing vastly improved bare-earth surfaces and feature extraction. Several advantages in object interpretation are gained when LIDAR data is combined with aerial imagery because both reflection properties and geometric information are observed. This paper deals with the fusion of return intensity data and aerial image data to improve the discovery of feature attributes from LIDAR points cloud. Return intensity measures provide information of laser reflectance characteristics of objects while aerial image data allows the identification of specific thermal conditions in the target area. By specifying ranges of aerial images, according to the objects' spectral analysis results, LIDAR point cloud may be filtered by its' color attributes. And through the analysis to the spatial patterns of return intensity of the filtered data, correlation between return intensity and object's attribute may be resulted in, and by their intensity attributes, LIDAR points cloud can be filtered with its intensity attributes.

2. MATERIALS

2.1 LIDAR instrument and its parameters

The LiteMapper-5600 system, integrating RIEGL LMS-Q560 laser scanner and IGI DigiCAM 22R/RI digital camera, is used in the data measurement. The DigiCAM is a medium-format airborne digital modular camera system for aerial image acquisition, which covers the same swath the LIDAR system sees providing high-resolution imagery of the surface in true color to aid surface classification and to provide extra planimetric resolution. And the key specifications of the RIEGL LMS-Q560 and IGI DigiCAM are listed in Tab1.

	RIEGL LMS-Q560	DigiCAM 22R/RI	
Laser wavelength	1550nm	Pixels	5400*4100
Laser beam divergence	≤0.5mrad	Sensor	CCD
Laser pulse repetition rate	240000hz	Frame rate	0.6s – 4s
High mean measurement rate	160khz		B:400-500
High ranging accuracy	20mm	Spectral channels	G:480-600
Scan angle range	±22.5deg		R:580-660

Table 1. Key specifications of the RIEGL LMS-Q560 and IGI DigiCAMs(RIEGL, 2007)

2.2 LIDAR data composition

The LIDAR data used in this paper, representing about 10km² area, including mainly buildings, asphalted concrete roads, vegetations, water and bare soil, were captured in March 2006 using the LiteMapper-5600 system mounted on a helicopter. And the helicopter flew at a nominal altitude of 1500m above ground with a scanning swath width of approximately 500m. The flying parameters resulted in a laser point sampling density averaging in the order of 2-3 pulses per square meter projected on the surface. The SILC image of raw LIDAR points and its DSM image are showed in Figure1. And from the SILC image (Figure1(a)), vegetation, grass land, road, buildings and water can be visible clearly.



(a) SILC image of the raw LIDAR points



(b) DSM image of the raw LIDAR points

Figure1: SILC image and DSM image of the raw LIDAR points

3. SPECTRAL REFLECTION OF CCD IMAGES AND LASER RETURN

3.1 Spectral reflectance of CCD images

The advantage of CCD images is its high quality in geometry and radiometry. In the CCD images from the camera in the LIDAR system, each pixel is represented by a digital number DN from 0 to 255 in either one of red, green or blue spectral. And the reflectance of the image scene is affected by not only the object's material composition and construction but also the sun-object-sensor geometry and atmospheric attenuation. And exploration has showed that shadow is an important factor to the radiation reflection in the image scene, there is considerable variation in brightness depending on the pixel position, e.g. tree crowns situated on the sun side of the image appear darker because the aerial sensor records greater portion of radiation reflected by the shadowed parts of the tree crowns. In general, vegetation, absorbing strongly at about 450nm and 670nm and reflects larger energy at about 520-600nm, has a higher DN value at green spectral; soil and asphalt concrete have rather higher values than that of the vegetations for almost all spectral regions. According to the spectral of DigiCAM camera, Table2 shows the equivalent reflectivity results for the typical spectral reflectance curve for the typical land-coverage in the region campaign obtained with the ASD instrument, and formula (1) shows the algorithm for the equivalent reflectivity. In which, asphalted concrete has the highest equivalent reflectivity values in three spectral regions; the equivalent reflectivity values for the grass, deciduous, conifer, construction asphalt can't be differentiated very clearly, and that of the sand is larger than that of the bare soil, and may be lighter in the CCD images.

$$\rho_{\lambda_1-\lambda_2} = \sum_{i=1}^n \rho_i / n \quad (1)$$

Where $\rho_{\lambda_1-\lambda_2}$ is the equivalent reflectivity between wavelengths λ_1 to λ_2 , and ρ_i is the sampling reflectivity between wavelengths λ_1 to λ_2 , n represents the sampling number.

Spectra Ranges(nm)	Red (580-660)	Green (480-600)	Blue (400-500)
Grass	0.0412	0.0794	0.0536
Deciduous	0.0589	0.0836	0.0502
Conifer	0.0489	0.0799	0.0465
Construction Asphalt	0.0548	0.0698	0.0841
Asphalted concrete	0.3583	0.1733	0.2076
Sand	0.1573	0.2394	0.3030
Bare soil	0.1207	0.1878	0.2432

Table2. Equivalent reflectivity of typical spectral reflectance of some land-coverage in the study area

3.2 Spectral reflectance of laser scanning

LIDAR data are acquired with just one band and the laser footprint is approximately circular and varies with the scan angle and the topography. The radiometric quality of LIDAR

data is inferior to that of the aerial images with LIDAR the signal can be very low especially for high flying heights and low reflectivity targets (Baltsavias, 1999). With pulse lasers the recorded intensity is in most cases not the integration of the returned echo but just its maximum, and the backscattering intensity is function of many variables as the laser power, the double distance source-target, the incidence angle, the reflectivity of the target, the media absorption, etc.. And one important advantage of laser intensity is that, being produced by active system; it is insensitive to illumination shadows. And according to the experiment by the RIEGL Company, under the conditions of perpendicular angle of incidence and average brightness, when the fault targets are larger than footprint of laser beam, the reflectivity of the targets in RIEGL LMS-Q560 is showed in Table3(RIEGL, 2007).

Objects	Target reflectivity (%)
Cliff, sand, masonry	60
Terra cotta	35
Vegetation	30
Dry asphalt	20
Coniferous trees	15
Dry snow	10
Wet ice	5

Table3: Objects reflectivity in RIEGL LMS-Q560

From Table2 and Table3, asphalted concrete, sand and bare soil have higher values at all three spectral ranges and higher laser returns reflectivity, which will make them show brighter pixels in the CCD images and larger intensity values in the intensity images, and an opposite situation happens to the vegetation and dry asphalt. The brightness and intensity differences can be as important clues for filtering the point cloud.

4. SPATIAL DISTRIBUTION ANALYSIS FOR THE INTENSITY AND SPECTRAL ATTRIBUTES OF THE POINT CLOUD

4.1 Data preprocess

As pulses hit reflective surfaces (glass, burnished metals, etc.) or anomalous interfaces (steam clouds, dust, smoke, etc.), some returns may experience refractive effects and cause coordinate value errors and therefore produce data static (noise). The first step was to graphically inspect the raw data for outliers that could be considered to be errors of data collection or processing, and the occasional point, completely remote from any neighboring height coordinates, should be removed. And that processing was completed with the terrasolid software.

4.2 DSM image of all returns point

The DSM elevation data is organized in a standardized tile scheme, and the resolution was selected to be 1-meter. As water

areas are always suspect and elevation values from these surfaces should not be considered valid.

4.3 Thematic images of intensity of all returns point

Intensity values are divided into six ranges; [0–40), [40–80), [80–120), [120–160), [160–200), [200–). And every returns point is classified with its intensity attribute. The resolution for the intensity image is selected to be 1-meter. Therefore, in its TIFF format the intensity information provides a panchromatic image of the return surface at the 1-meter pixel resolution. Intensity values vary depending from which type of surface the return point reflection is obtained and this translates into a series of tonal differences.

4.4 reflectivity thematic images of range of red, green and blue

SILC (Spectral Image LIDAR Composite) is the application of RGB values (0-255) to LIDAR point records. After the SILC process, LIDAR data is fused with spectra data and every laser returns point has three ranges of spectra attributes (DN values).

And by specifying ranges of red, green and blue, SILC data may be filtered by the color attributes. The DN values of the three spectra are from 0 to 255, which are divided into six ranges; [0–20), [20–80), [80–100), [100–150), [150–200) and [200, 255]. And three reflectivity thematic images with TIFF format are produced, and resolutions of the three range of thematic reflectivity images are all equal to 1-meter.

4.5 reflectance spatial distribution of return points and CCD images

The number of points in the experiment LIDAR data is 414846. And from the return intensity diagram showed in Figure2, scaled intensity values for all returns are from 14 to 255, of which the histogram shows a continuous but asymmetric distribution. But in the attribute table for all the returns point, the maximum scaled intensity value is 8987, and the number of points with intensity larger than 255 is 695, less than 0.17% of the all return number, the little number of returns point may be the reason why the number of returns point with scaled intensity larger than 255 not showed in the diagram.

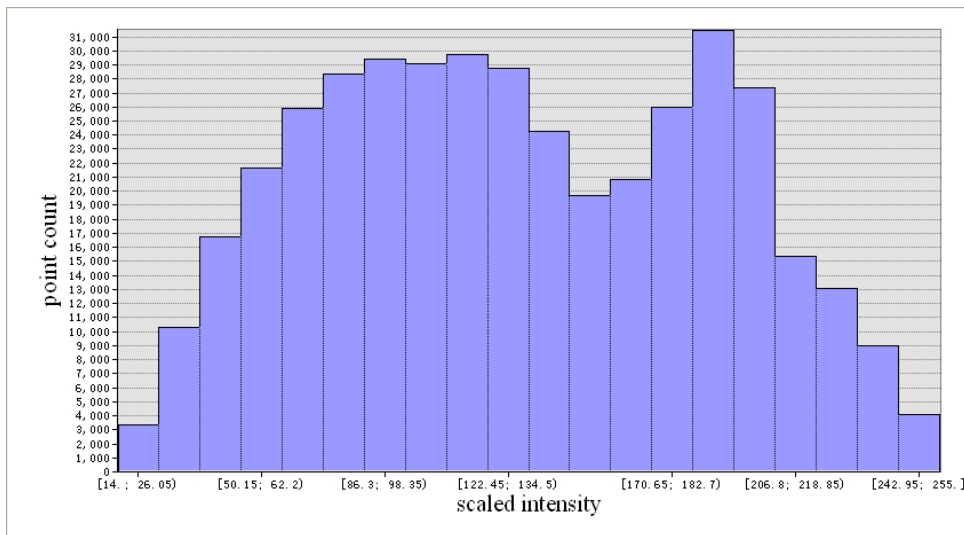
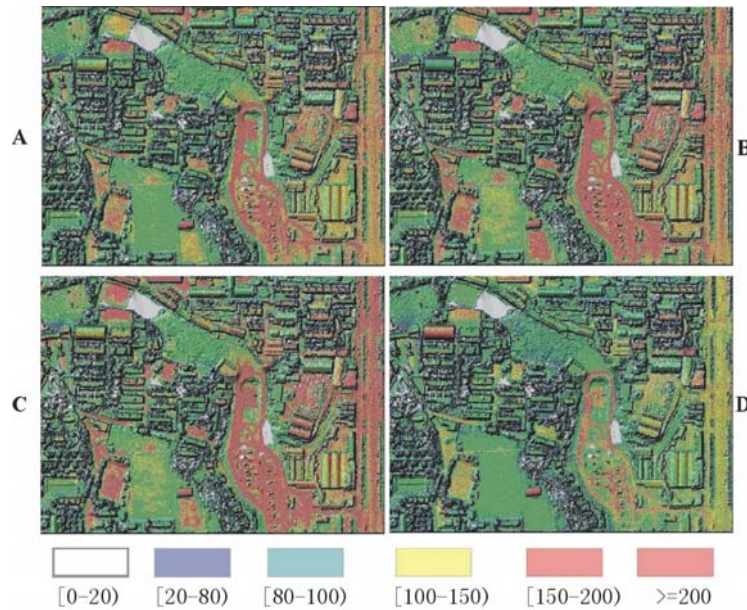


Figure2: all return intensity diagram

4.6 overlapping analyses of intensity and spectra thematic images on the DSM

Distributions of intensity and the digital numbers images are overlapped on the DSM images, and the distributions of the intensity and reflection digital numbers of the aerial images in

study area are presented in Figure3; A (intensity image), b (DN images of red range), c (DN images of green range) and d (DN images of blue range). The overlapping results interpret a strong similar relation of spatial distribution among objects and their intensity and spectral DN.



(A: returns intensity; B: red spectra; C: green spectra; D: blue spectra)

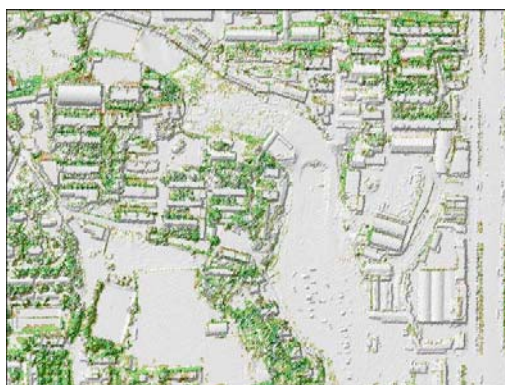
Figure3: overlaying digital elevation mode with intensity distribution map

5. FILTERING RETURN POINTS BY DN AND INTENSITY ATTRIBUTES

5.1 Filtering LIDAR point by DN values

According to the overlapping results of intensity and spectra thematic images on the DSM, exposed soil have largest digital number DN in spectra of red, green and blue, and the digital number DN in red, green and blue spectra for grass and construction asphalt are larger than that of the surrounding vegetation, and exhibit a “lighter” color properties. This analysis provides a solution to separate data by color allows the

“lighter” points to be gently filtered and the darker terrain to be filtered more aggressively. This method will be useful in filtering the points in steep topographic terrain, in which it is difficult to treat with conventional filters because trees and high vegetation have spatial properties similar to boulders. Figure4 shows the filtering results by three DN properties. The corresponding DN parameters for the vegetation filtering are 0-80, 20-100, and 0-80 separately, and with which 71188 points are filtered; the DN parameters for the bare soil and construction asphalt are 150-255, 150-255 and 150-255, and 102301 points are filtered.



A: intensity distribution of the filtered vegetation’s returns B: intensity distribution of the filtered bare soil and asphalt concrete

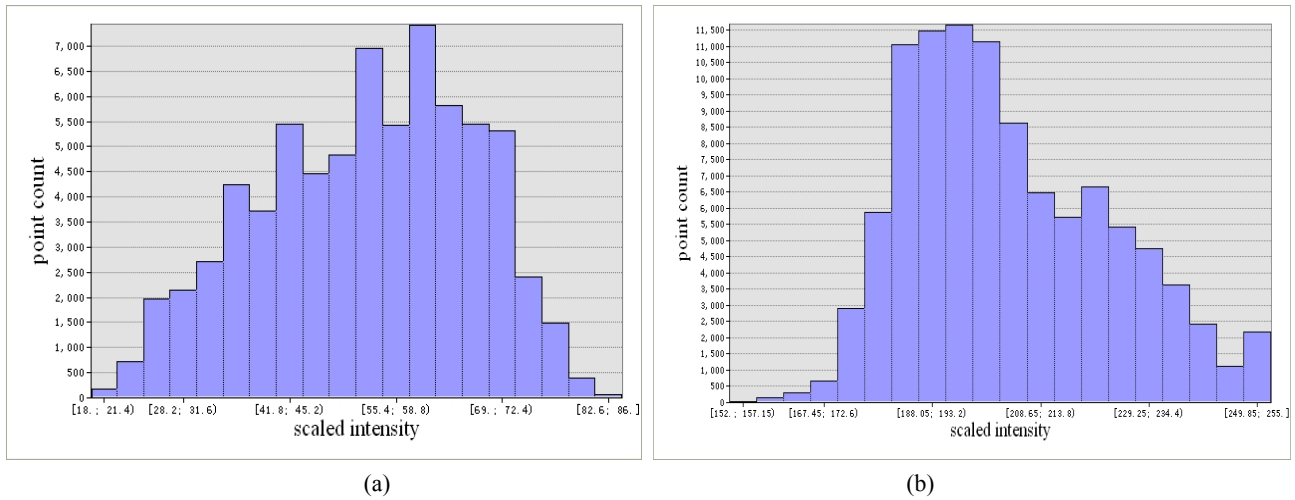
Figure4. Intensity distribution of the filtered vegetation’s returns by RGB attributes

5.2 Intensity distribution of the filtered points by RGB parameters

The diagrams of the scaled intensity distribution of filtered vegetation and bare soil and asphalt concrete are showed in Figure5, in which the intensity value scope of filtered vegetation is 18-86, mainly in 21-80, and the range of the

filtered bare soil and asphalt concrete is 152-255, mainly in 172-255, which shows a strong intensity characteristic for

different objects.



(a: intensity diagram of the filtered vegetation; b: intensity diagram of the filter bare soil and asphalt concrete)

Figure5. Scaled intensity diagrams of filtered returns point

5.3 Filter point cloud by intensity measures

For the luminance and other impacts on the DN of targets spectral reflection, there is considerable variation in brightness depending on the pixel position and many vegetation points will not be filtered. And one important advantage of laser intensity is that it is insensitive to illumination shadows.

Therefore returns point can be filtered by intensity properties according to the diagram of DN parameter filtering results. And the filtering results are showed in figure6, in which the numbers of filtered points are 35270 for vegetation and 59560 for bare soil in the other set of pints. And the unfiltered return points are showed in the Figure6.

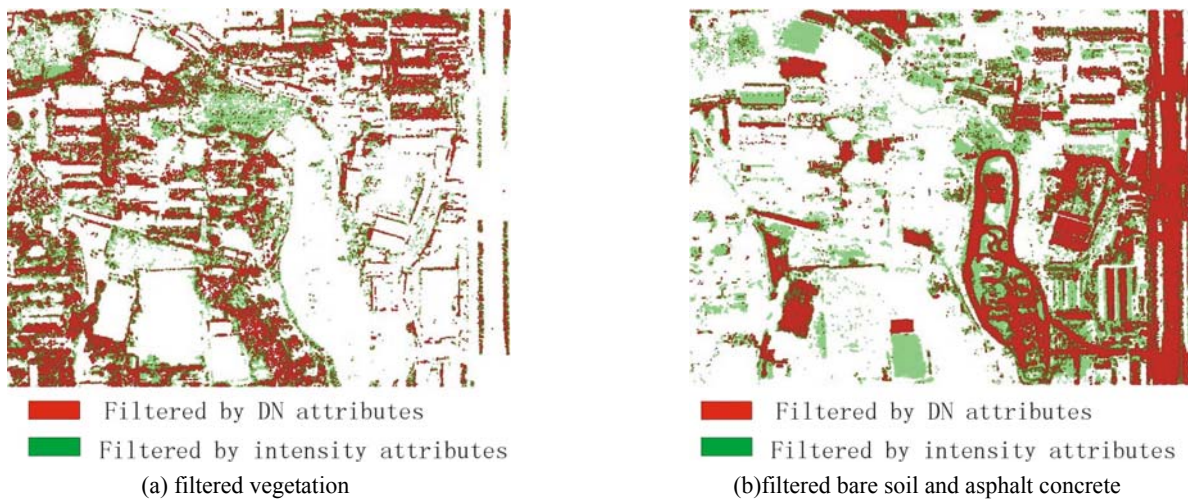


Figure6 filtered return points

6. DISCUSSION AND CONCLUSION

This study is intended to show a possibility and a method to filtering LIDAR points by fusing of return intensity and spectra DN of aerial images. By fusion of return points cloud with the accurate spectral aerial images provided by aerial cameras on the same board, the laser return points can get both intensity and spectra digital number attributes. And the spatial distribution of returns intensity and DN of the three spectral

ranges of aerial images are both similarity to the distribution of objects for typical land-coverage. The filtered return points by the DN and intensity method are also relatively in the spatial distribution, which interprets that intensity and spectra DN of aerial images are both important information in the feature extraction for the LIDAR data. With three spectra DN of aerial images, LIDAR points can be filtered by indexes of brightness, but the quality is impacted by illumination factors; however, insensitive to illumination shadows, the returns intensity

attributes can be compensation to the indexes of brightness in the filtering process. This is the reason why most of the filter vegetation lies at one side of the vegetation filtered by DN attributes (showed in Figure6(a)).

The key and difficult to filter returns points by spectra DN is how to get the accurate ranges of DN. In this paper, by comparing the equivalent reflectivity of typical land-coverage and overlapping the DN distribution images on the DSM of the raw return points, the ranges of the DN are determinate. And with the complexity of radiation reflectivity in the aerial images, the unavoidable errors in the filtering by range of DN will bring errors to the statistics of the filtered features intensity. And the correlation between the scope of DN and intensity for a special feature are still unavailable, which should be a key knowledge to the filtering method in this paper.

ACKNOWLEDGEMENTS

This study was supported by the National Science Foundation of China (40401050) and the Science Foundation of Shanghai Education department (07ZZ09).

REFERENCE

Ahokas, E., Kaasalainen, S., Hyypää, J., Suomalainen, J., 2006. Calibration of the Optech ALTM 3100 laser scanner intensity data using brightness targets. *International Archives of Photogrammetry, Remote Sensing and Spatial Information Sciences* 36 (Part 1). on CDROM.

Baltsavias, E.P., 1999. Airborne laser scanning: basic relations and formulas. *ISPRS Journal of Photogrammetry and Remote Sensing* 54 (2–3), 199–214.

Bernhard Höfle, Norbert Pfeifer, 2007, Correction of laser scanning intensity data: Data and model-driven approaches. *ISPRS Journal of Photogrammetry & Remote Sensing*, 61, 1-19

Emmanuel P. Baltsavias, 1999, A comparison between photogrammetry and laser scanning, *ISPRS Journal of Photogrammetry & Remote Sensing*, 54, 83–94

Holmgren, J., Persson, A., 2004. Identifying species of individual trees using airborne laser scanner. *Remote Sensing of Environment*, 90, 415–423.

Jeong-Heon Song, Soo-Hee Han, Kiyun Yu, Yong-Il Kim, 2006, Assessing The Possibility of Land-cover Classification Using LIDAR Intensity Data. <http://www.isprs.org/commission3/proceedings02/papers/paper128.pdf>. accessed April 3, 2007

Johan Holmgren, Asa Persson. 2004, Identifying species of individual trees using airborne laser scanner. *Remote Sensing of Environment*, 90, 415–423

Jonas, D., 2002. Airborne laser scanning: developments in intensity and beam divergence. *Proceedings of the 11th Australasian Remote Sensing and Photogrammetry Conference* September, Brisbane, Australia.

Kim, I.I., McArthur, B., Korevaar, E., 2001. Comparison of laser beam propagation at 785 nm and 1550 nm in fog and haze for optical wireless communications. *Proceedings of SPIE, The International Society for Optical Engineering*, 4214, 26–37.

Lim, K., Treitz, P., Baldwin, K., Morrison, I., Green, J., 2003. Lidar remote sensing of biophysical properties of tolerant northern hardwood forests. *Canadian Journal of Remote Sensing*, 29 (5), 658–678.

RIEGL, 2007, Airborne laser scanner LMS-Q560 for full waveform analysis. http://www.riegl.com/airborne_scanners/airborne-scanner-packages/pdf_airbone-laser-scanner-packages/lms-q560_datasheet.pdf. accessed September 27, 2007

RIEGL, 2007, specifications digicam h39. http://www.igi-systems.com/downloads/specifications/specifications_digicam_h39.pdf. accessed September 29, 2007

Schreier, H., Lougheed, J., Tucker, C., Leckie, D., 1985. Automated measurements of terrain reflection and height variations using an airborne infrared laser system. *International Journal of Remote Sensing* 6 (1), 101–103.

T. Moffieta, K. Mengersenb, C. Wittec, R. Kinga, R. Denham. 2005, Airborne laser scanning: Exploratory data analysis indicates potential variables for classification of individual trees or forest stands according to species. *ISPRS Journal of Photogrammetry & Remote Sensing*, 59, 289–309

Tomas Brandtberg. 2007, classifying individual tree species under leaf-off and leaf-on conditions using airborne lidar. *ISPRS Journal of Photogrammetry & Remote Sensing*, 61, 325–340

